



Bidirectional Power Flow Control using CLLC Resonant Converter for DC Distribution System

K.Ramya, R.Sundaramoorthi., ME (PhD)

PG Student, Dept. of EEE, Kings College of Engineering, Thanjavur, Tamilnadu, India¹

Assistant professor, Dept. of EEE, Kings College of Engineering, Thanjavur, Tamilnadu, India²

ABSTRACT: A single-phase bi-directional CLLC resonant converter with dc-bus voltage regulation and power compensation is proposed for dc distribution applications. This converter can be operated in both buck and boost mode. In the presence of dc bus, the battery is being charged and in the absence of the dc bus the battery supplies power. A suitable control circuit is presented to improve the power conversion efficiency and reduces the switching loss of the conventional isolated bidirectional ac-dc converter. The ZVS operation of the primary power IGBTs and the soft commutation of the output rectifiers are significant factors for the efficiency-optimal design of the bidirectional full-bridge CLLC resonant converter. Finally simulation results for boost and buck modes of CLLC resonant converter is obtained.

KEYWORDS: Bidirectional DC/DC converter, current stress, micro grid, phase-shift control, power distribution, power flow.

I. INTRODUCTION

With the increasing demands for electric power in future automobiles, uninterrupted power supplies (UPSs), renewable energy sources, telecom and computer systems, and aviation power systems, bidirectional dc-dc converters (BDCs) exhibit as an ever-lasting key component to interface between a high-voltage bus where an energy generation device such as a fuel cell stack and/or a photovoltaic array is installed, and a low-voltage bus, where usually an energy storage device such as a battery or a super capacitor is implemented, to actively provide clean and stable power and to enable high reliability, effectiveness, and maneuverability of the power systems aforementioned [1]. In order to significantly reduce reactive component size and cost, high-frequency operation of BDCs is desirable. However, in a hard-switching converter, as the switching frequency increases, switching losses and electromagnetic interference increase. To resolve this problem, soft-switching converters are employed.

Several isolated BDC topologies have been suggested for applications of the dc power distribution systems. A boost full-bridge ZVS PWM dc-dc converter was developed for bidirectional high power applications using passive [2], lossless [3], and fly back [4] snubbers. This topology is proper to the bidirectional power conversion because it has a boost mode for low to high voltage power conversion and a buck mode for vice versa. However, this topology requires a snubber circuit to suppress the voltage stress of the switches, which increases circuit complexity and decreases power conversion efficiency. A bidirectional phase shift full-bridge converter was proposed with high frequency galvanic isolation for energy storage systems [5], [6]. This converter can improve power conversion efficiency using a zero voltage transition (ZVT) feature; however, it requires input voltage variations to regulate constant output voltage because this topology can only achieve the step-down operation. This paper presents such a minimized switching loss BDC. The soft switching feature for the proposed converter is realized only by a very simple CLLC resonant tank. In the proposed system without any other additional soft-switching auxiliary circuits and being snubberless, the overall component count can be dramatically reduced. The operation principles and experimental results of the proposed converter is described.

International Journal of Advanced Research in Electrical, Electronics and Instrumentation Engineering

(An ISO 3297: 2007 Certified Organization)

Vol. 3, Issue 4, April 2014

II. OVERVIEW OF RESONANT CONVERTER

Resonant converters use a resonant circuit for switching the transistors when they are at the zero current or zero voltage point, this reduces the stress on the switching transistors and the radio interference. To control the output voltage, resonant converters are driven with a constant pulse duration at a variable frequency. The pulse duration is required to be equal to half of the resonant period time for switching at the zero-crossing points of current or voltage. There are many different types of resonant converters. For example the resonant circuit can be placed at the primary or secondary side of the transformer. Another alternative is that a serial or parallel resonant circuit can be used, depending on whether it is required to turn off the transistor, when the current is zero or the voltage is zero. Since the converter is controlled through frequency modulation, the impedance of the resonant network will be changed by changing the switching frequency in response to load changes. Consequently the output voltage can be regulated by changing impedance of the resonant tank circuit. For example, if the load current increases the output voltage will have a tendency to decrease. The feedback circuit will sense this decrease and move the switching frequency of the converter toward resonance such that more voltage applied to the resonant network will be dropped across the load thereby increasing the output voltage.

Conversely, if the load current decreases, the feedback circuit will move the frequency away from resonance such that more voltage is dropped across the tank circuit. The fact that the converter works as a voltage divider means that the maximum gain that can be achieved in the power train of the converter is one. The advantage of the series resonant converter is that it can zero voltage the main switches, Q1 and Q2, in Figure 1. This improves the efficiency of the converter particularly as higher switching frequencies are used.

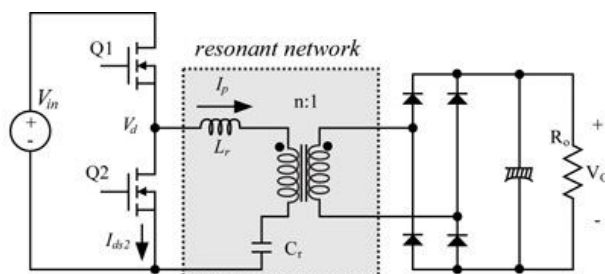


Fig 1: Series Resonant Converter

III. CIRCUIT DESCRIPTION OF PROPOSED SYSTEM

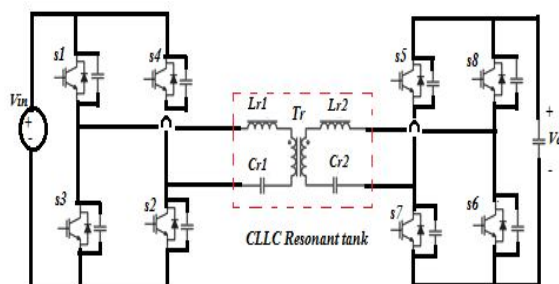


Fig 2: Bidirectional full bridge CLLC resonant converter



International Journal of Advanced Research in Electrical, Electronics and Instrumentation Engineering

(An ISO 3297: 2007 Certified Organization)

Vol. 3, Issue 4, April 2014

In the proposed system DC voltage is given to the primary inverting stage. CLLC Resonant tank has two capacitances Cr1 and Cr2 for automatic flux balance. It also has two inductance Lr1 and Lr2 for achieving high resonant frequency. IGBTs operate under ZVS condition with minimum switching loss when compared to the conventional system. For soft commutation of the output rectifiers switching frequency must be less than resonant frequency. Turn-on or turn-off transitions of semiconductor devices can occur at zero crossings of tank voltage or current waveforms, thereby reducing or eliminating some of the switching loss mechanisms. Hence resonant converters can operate at higher switching frequencies than comparable PWM converters Zero-voltage switching also reduces converter-generated EMI. Zero-current switching can be used to commutate the switches. In specialized applications, resonant networks may be unavoidable. High voltage converters have significant transformer leakage inductance and winding capacitance leads to resonant network. The primary and secondary windings of the transformer may be used to step up or step down the voltage output. So, it can be made in such a way that a 120 V load can match a 208V load. Isolation transformers which have the Faraday shield will have improved power quality because of attenuated higher frequency noise currents. The Faraday shield also decreases the leakage current of the equipment and the isolator below 300 microamps. They help in giving a better impedance matching of a critical load to an electrical circuit.

A. SOFT-SWITCHING CONDITIONS

The ZVS operation of the primary power IGBTs and the soft commutation of the output rectifiers are significant factors for the efficiency-optimal design of the bidirectional full-bridge CLLC resonant converter. The lower operating frequency than the resonant frequency can guarantee the soft commutation of the output rectifiers because the difference between the switching frequency and the resonant frequency makes discontinuous rectifying current. In addition, during the dead time of the switches, the primary current should discharge the output capacitance of four primary switches for their ZVS turn-on.

$$tdt \geq 4Vd \cdot \max\{Cs1, Cs2, Cs3, Cs4\} = 16Cs_{fs, \max} Lm$$

$$\min\{ |ip(ta) | , ip(td) \} \tag{1}$$

$$fs \leq fr \tag{2}$$

$$Lm \leq \frac{tdt}{16 Cs_{fs, \max}} = \frac{tdt}{16Cs fr} \tag{3}$$

IV. DIGITAL CONTROL SCHEME FOR BIDIRECTIONAL OPERATION

Bidirectional power converters require a mode change algorithm to select their power conversion direction. This power conversion mode should be selected considering the direction of the power flow in the converter. The direction of the power flow will be easily detected if there is a current sensor connected between the converter's output capacitor and load side. However, it can decrease the flexibility of the bidirectional power conversion system since the current information has to contain the power flow direction of the entire load. It means that if the proposed system is expanded to a multiple module system connected in parallel, additional and huge current sensors will be required to obtain the power flow information for the entire load. To avoid this problem, a dead-band control algorithm is proposed to smoothly change the power conversion direction only using output voltage information. When the load becomes negative, the output voltage of the converter Fig.3(a) shows the theoretical waveforms of the proposed dead-band control algorithm for the bidirectional CLLC resonant converter. When the load becomes negative, the output voltage of the converter will drastically increase because power is supplied to the output capacitor from two sides: the converter side and the load side. At this time, the converter is uncontrollable without changing the power conversion mode because of the negative power flow. If the output voltage reaches the positive dead-band voltage $+V_{band}$, the power conversion mode changes from the powering mode to the generating mode. In this generating mode, the converter

International Journal of Advanced Research in Electrical, Electronics and Instrumentation Engineering

(An ISO 3297: 2007 Certified Organization)

Vol. 3, Issue 4, April 2014

transfers power from load to input side. Then, the output voltage will decrease to the reference voltage V_{ref} , which will be regulated by a pulse frequency modulation (PFM) controller. In the same manner, the power conversion mode can be changed from the generating mode to the powering mode.

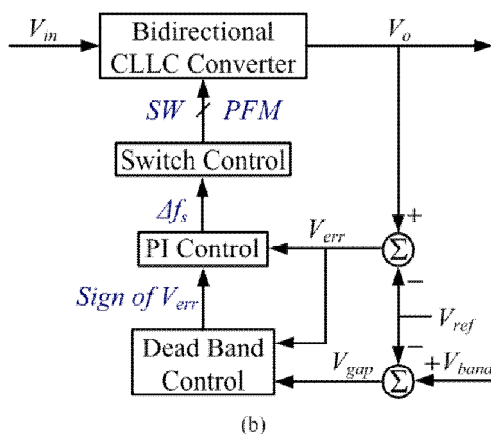
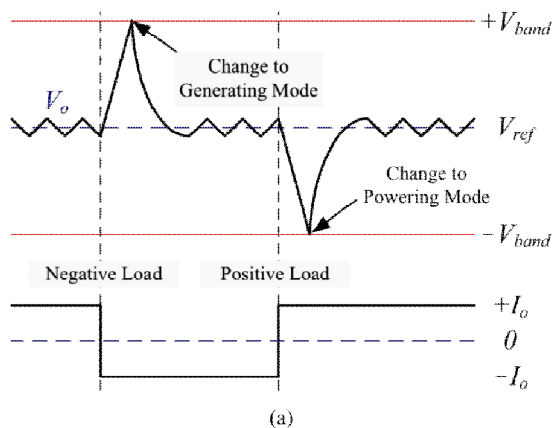


Fig 3: Schematic of proposed dead band control algorithm

When the load becomes positive, the output voltage will decrease to the negative dead-band voltage $-V_{band}$. Then, the power conversion mode is changed and the output voltage will increase to V_{ref} . Fig.3(b) shows the block diagram of the proposed digital controller. The dead-band controller can select the power conversion mode using the voltage gap V_{gap} which is the voltage difference between the output voltage and the dead-band voltage. This dead-band controller generates the sign of the voltage error V_{err} which is the voltage difference between the output voltage and the reference voltage. The PI controller regulates the output voltage using V_{err} and its sign. The switch control block generates PFM switching pulses using the calculated.

V. OPERATIONAL PRINCIPLE

In Mode 1, which is a dead-time duration, there is no power transferred to the secondary rectifying stage. The primary current charges the output capacitance of the primary switches S3 and S4, and discharges the output capacitance of S1 and S2. After the charge and discharge processes, the primary current will pass through the antiparallel diode of S1 and S2, which makes the switches operate under the ZVS condition. In Mode 2, S1 and S2 turn on and power will be transferred to the secondary rectifying stage through the transformer Tr.

International Journal of Advanced Research in Electrical, Electronics and Instrumentation Engineering

(An ISO 3297: 2007 Certified Organization)

Vol. 3, Issue 4, April 2014

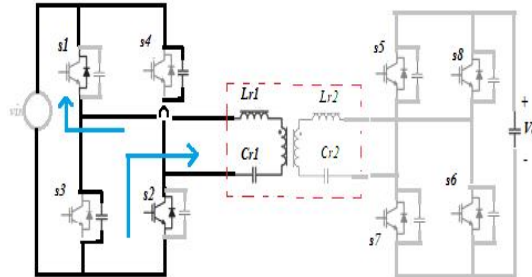


Fig 4: Boost mode operation of bidirectional converter:
 Mode (1)

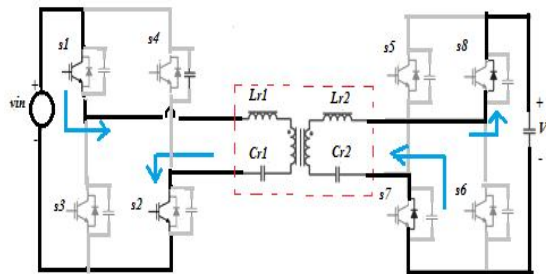


Fig 5: Mode (2)

The primary current changes its direction to positive according to S1 and S2 because the input voltage source V_{in} forces the primary current to the positive direction through S1 and S2. Mode 2 will end when the primary current i_p meets the magnetizing current i_m , which means the end of the resonance operation transferring power from the primary to secondary stage. This operation will repeat in Mode 4 and 5 with the same manner. Mode 4 and 5 repeat the ZVS operation of S3 and S4 and power transfer from the primary to secondary stage using the resonance operation.

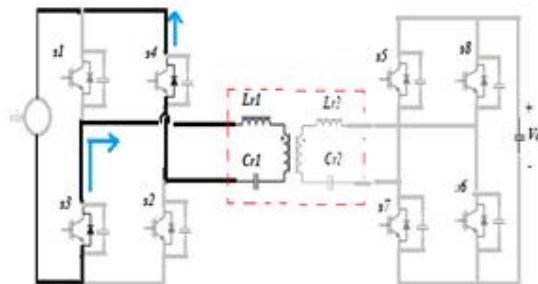


Fig 6: Mode (3)

International Journal of Advanced Research in Electrical, Electronics and Instrumentation Engineering

(An ISO 3297: 2007 Certified Organization)

Vol. 3, Issue 4, April 2014

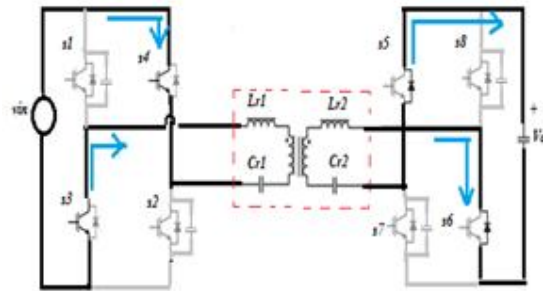


Fig 7: Mode (4)

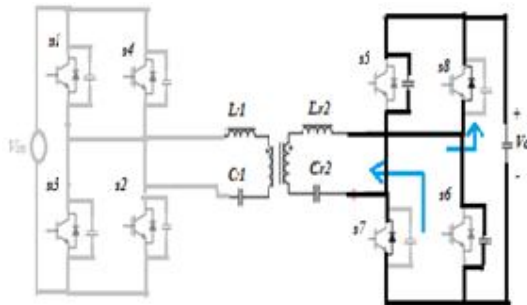


Fig 8 :Buck mode operation of bidirectional converter

Mode(1)

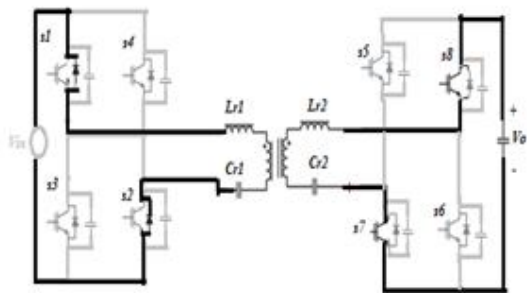


Fig 9: Mode(2)

Similarly in buck mode operation power flow is from secondary to primary side. The capacitor discharges the stored energy from load to source thereby contributes power flow in reverse direction. Simulation results show smooth transition of power flow in both the directions. When compared to conventional system it has reduced switching losses since the switches are operated in ZVS condition.



International Journal of Advanced Research in Electrical, Electronics and Instrumentation Engineering

(An ISO 3297: 2007 Certified Organization)

Vol. 3, Issue 4, April 2014

TABLE I

DESIGN SPECIFICATION:

Parameter		Value [Unit]
Rated Power	P_{max}	4 [kW]
- Maximum Input Voltage	$V_{in,max}$	110 Vdc
- Minimum Input Voltage	$V_{in,min}$	80 Vdc
Input Voltage Frequency	$V_{in,freq}$	50 [Hz]
Output Power Range	P_{max}	8000-10,000[w]
Input Current Range	$I_{in,max}$	9 [A _{rms}]
Output Voltage Range	$V_{out,dc}$	370-570[V _{dc}]
Output Current Range	$I_{out,dc}$	16-20 [A _{dc}]

VI. SIMULATION RESULTS

A. BOOST MODE

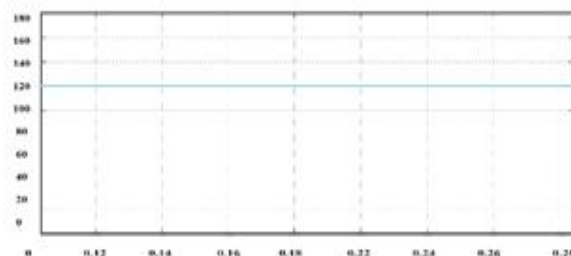


Fig 10. Input voltage

In fig 10 shows the graph of input DC voltage given to the bidirectional converter at the primary side.

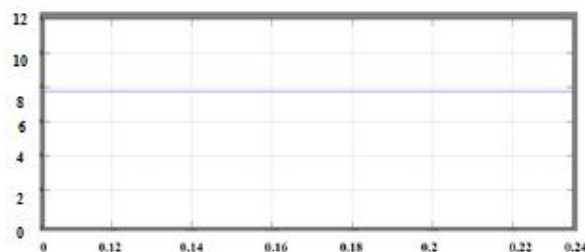


Fig 11. Input current

Fig 11 shows the input current of 8 A given at the primary side of the switches.



International Journal of Advanced Research in Electrical, Electronics and Instrumentation Engineering

(An ISO 3297: 2007 Certified Organization)

Vol. 3, Issue 4, April 2014



Fig 12. Switching pluses

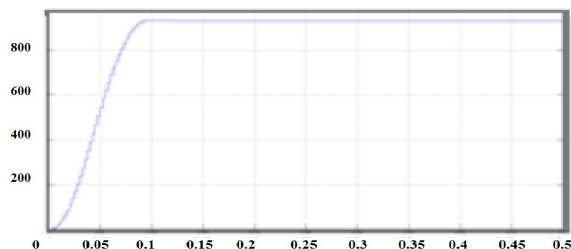


Fig 13. Output voltage

The waveforms of the drain-source voltage of S1, the primary and secondary current, and the output voltage are illustrated in fig12 and fig 13 respectively. In Fig. 13, the distortion level of the output voltage regulation is almost 8V at the step load variations from 0.75kW to 4.25kW and vice versa. All waveforms are measured in the powering mode; however, the generating mode has also the same waveforms because of the converter's symmetric structure.

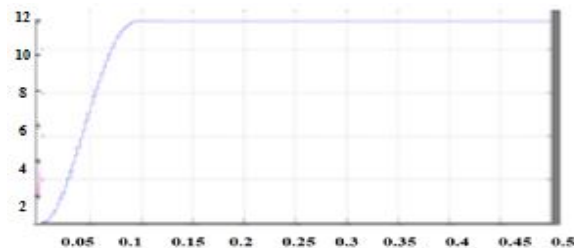


Fig 14. Output current

The current waveforms show that the ZVS of the primary switches and soft commutation of the secondary rectifiers are well achieved at the minimum and rated load conditions.

B. BUCK MODE

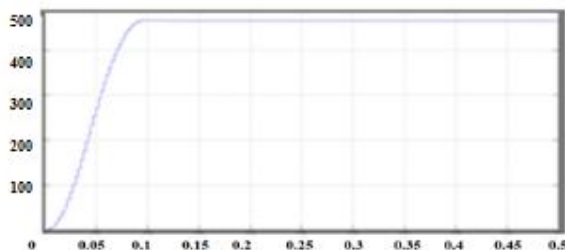


Fig 15. Output voltage



International Journal of Advanced Research in Electrical, Electronics and Instrumentation Engineering

(An ISO 3297: 2007 Certified Organization)

Vol. 3, Issue 4, April 2014

Fig. 13 and 15 show experimental waveforms of the step load response of the proposed converter in the case of the bidirectional power conversion, ie.boost and buck mode respectively. In Fig. 15, the distortion level of the output voltage is around 10V for the mode change of the power conversion direction because the dead-band voltage V_{band} is set to 10V in the controller.

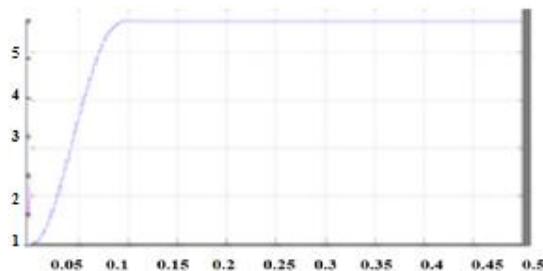


Fig 16. Output current

Compared to Fig.12, the experimental waveform of the mode change verifies that the proposed dead-band controller is well designed to change the power flow of the converter smoothly. This efficiency curve shows that the proposed bidirectional CLLC resonant converter has a good efficiency characteristic under middle and high load conditions. The maximum power conversion efficiency of the prototype converter is 97.8% at 4kW. It is noted that the power conversion efficiency of the reverse power flow is exactly the same as the measured data because the structure of the converter's power stage is symmetric with respect to the primary inverting and secondary rectifying stages.

VII. CONCLUSION

A bidirectional DC-DC converter for distributed generation application has been designed, simulated. Mathematical models for the buck and boost modes of the DC-DC converter are derived. An average model for the DC to DC converter is obtained using MATLAB Simulink. It is observed that the current change its direction quickly as the mode of operation changes without any overshoot of the values. Hence, the converter's voltage and current are stable in its operation in both directions. The DC-DC converter design has been tested by computer simulation using R and RL load. The soft-switching condition of the converter is derived to obtain the design methodology of the resonant network. In addition, the dead-band and switch transition control algorithms are proposed to smoothly change the power flow direction in the converter.

REFERENCES

- [1] G.-S. Seo, J. Baek, K. Choi, H. Bae, and B. Cho, "Modeling and analysis of dc distribution systems," in *Proc. IEEE 8th Int. Conf. Power Electron. ECCE Asia*, May 2011, pp. 223–227.
- [2] K. Techakittiroj and V. Wongpaibool, "Co-existence between ac-distribution and dc-distribution: In the view of appliances," in *Proc. 2nd Int. Conf. Comput. Electrical Eng.*, Dec. 2009, vol. 1, pp. 421–425.
- [3] A. Stupar, T. Friedli, J. Minibock, and J. Kolar, "Towards a 99% efficient three-phase buck-type PFC rectifier for 400-V dc distribution systems," *IEEE Trans. Power Electron.*, vol. 27, no. 4, pp. 1732–1744, Apr. 2012.
- [4] T.-F. Wu, C.-L. Kuo, K.-H. Sun, and Y.-C. Chang, "DC-busvoltage regulation and power compensation with bi-directional inverter in dc-microgrid applications," in *Proc. IEEE Energy Convers. Congr. Expo.*, Sep. 2011, pp. 4161–4168.
- [5] B.-R. Lin and Z.-L. Hung, "A single-phase bidirectional rectifier with power factor correction," in *Proc. IEEE Energy Convers. Congr. Expo.*, Aug. 2001, vol. 2, pp. 601–605.
- [6] Y. Zhangang, C. Yanbo, and W. Chengshan, "Construction, operation and control of a laboratory-scale microgrid," in *Proc. Int. Conf. Sustainable Power Generation Supply*, Apr. 2009, pp. 1–5.
- [7] W. Ryckaert, K. De Gussemé, D. Van de Sype, L. Vandeveldel, and J. Melkebeek, "Damping potential of single-phase bidirectional rectifiers with resistive harmonic behaviour," *IEE Electric Power Appl.*, vol. 153, no. 1, pp. 68–74, Jan. 2006.
- [8] T.-F. Wu, K.-H. Sun, C.-L. Kuo, and C.-H. Chang, "Predictive current controlled 5-kW single-phase bidirectional inverter with wide inductance variation for dc-microgrid applications," *IEEE Trans. Power Electron.*, vol. 25, no. 12, pp. 3076–3084, Dec. 2010.
- [9] D. Dong, F. Luo, D. Boroyevich, and P. Mattavelli, "Leakage current reduction in a single-phase bidirectional ac-dc full-bridge inverter," *IEEE Trans. Power Electron.*, vol. 27, no. 10, pp. 4281–4291, Oct. 2012.



ISSN (Print) : 2320 – 3765
ISSN (Online): 2278 – 8875

International Journal of Advanced Research in Electrical, Electronics and Instrumentation Engineering

(An ISO 3297: 2007 Certified Organization)

Vol. 3, Issue 4, April 2014

- [10] K.H.Edelmoser and F.A.Himmelstoss, "Bidirectional dc-to-dc converter for solar battery backup applications," in *Proc. IEEE 35th Annu. Power Electron. Spec. Conf.*, Jun. 2004, vol. 3, pp. 2070–2074.
- [11] D. Salomonsson, L. Soder, and A. Sannino, "Protection of low-voltage dc microgrids," *IEEE Trans. Power Del.*, vol. 24, no. 3, pp. 1045–1053, July 2009.
- [12] J. Rekola and H. Tuusa, "Comparison of line and load converter topologies in a bipolar LVDC distribution," in *Proc. 14th Eur. Conf. Power Electron. Appl.*, Aug./Sep. 2011, pp. 1–10.
- [13] B. Zhao, Q. Yu, and W. Sun, "Extended-phase-shift control of isolated bidirectional dc-dc converter for power distribution in microgrid," *IEEE Trans. Power Electron.*, vol. 27, no. 11, pp. 4667–4680, Nov. 2012.
- [14] R. Mirzahosseini and F. Tahami, "A phase-shift three-phase bidirectional series resonant dc/dc converter," in *Proc. 37th Annu. Conf. IEEE Electron. Soc.*, Nov. 2011, pp. 1137–1143.
- [15] W. Li, H. Wu, H. Yu, and X. He, "Isolated winding-coupled bidirectional ZVS converter with PWM plus phase-shift (PPS) control strategy," *IEEE Trans. Power Electron.*, vol. 26, no. 12, pp. 3560–3570, Dec. 2011.
- [16] K. Wu, C. de Silva, and W. Dunford, "Stability analysis of isolated bidirectional dual active full-bridge dc-dc converter with triple phase-shift control," *IEEE Trans. Power Electron.*, vol. 27, no. 4, pp. 2007–2017, Apr. 2012.
- [17] W. Chen, P. Rong, and Z. Lu, "Snubberless bidirectional dc-dc converter with new CLLC resonant tank featuring minimized switching loss," *IEEE Trans. Ind. Electron.*, vol. 57, no. 9, pp. 3075–3086, Sep. 2010.
- [18] J.-H. Jung, H.-S. Kim, J.-H. Kim, M.-H. Ryu, and J.-W. Baek, "High efficiency bidirectional LLC resonant converter for 380 V dc power distribution system using digital control scheme," in *Proc. 27th Annu. IEEE Appl. Power. Electron. Conf.*, Feb. 2012, pp. 532–538.
- [19] T. Thacker, D. Boroyevich, R. Burgos, and F. Wang, "Phase-locked loop noise reduction via phase detector implementation for single-phase systems," *IEEE Trans. Ind. Electron.*, vol. 58, no. 6, pp. 2482–2490, Jun. 2011.
- [20] F. D. Freijedo, A. G. Yepes, O. Lopez, P. Fernandez-Comesana, and J. Doval-Gandoy, "An optimized implementation of phase-locked loops for grid applications," *IEEE Trans. Instrum. Meas.*, vol. 60, no. 9, pp. 3110 – 3119, Sep. 2011.
- [21] B. Meersman, J. D. Kooning, T. Vandoorn, L. Degroote, B. Renders, and L. Vandeveld, "Overview of PLL methods for distributed generation units," in *Proc. 45th Int. Univ. Power Eng. Conf.*, 2010, pp. 1–6.